

October 12, 2018

On the Break in the *Fermi*-LAT Spectrum of 3C 454.3

Justin D. Finke¹ and Charles D. Dermer

*U.S. Naval Research Laboratory, Code 7653, 4555 Overlook Ave SW, Washington, DC,
20375-5352*

¹*NRL/NRC Research Associate*

justin.finke@nrl.navy.mil

ABSTRACT

Fermi Gamma ray Space Telescope observations of the flat spectrum radio quasar 3C 454.3 show a spectral-index change $\Delta\Gamma \cong 1.2 \pm 0.3$ at break energy $E_{br} \approx 2.4 \pm 0.3$ GeV. Such a sharp break is inconsistent with a cooling electron distribution and is poorly fit with a synchrotron self-Compton model. We show that a combination of two components, namely the Compton-scattered disk and broad-line region (BLR) radiations, explains this spectral break and gives a good fit to the quasi-simultaneous radio, optical/UV, X-ray, and γ -ray spectral energy distribution observed in 2008 August. A sharp break can be produced independent of the emitting region's distance from the central black hole if the BLR has a gradient in density $\propto R^{-2}$, consistent with a wind model for the BLR.

Subject headings: gamma rays: galaxies — Quasar: 3C 454.3 — radiation mechanisms: non-thermal

1. Introduction

The flat spectrum radio quasar (FSRQ) 3C 454.3 (PKS 2251+158) is representative of blazars with large, $\gtrsim 10^{48}$ erg s⁻¹ apparent γ -ray luminosities, and is one of the brightest sources seen with the recently launched *Fermi* Gamma-Ray Space Telescope (Tosti et al. 2008; Escande & Tanaka 2009). It has also been detected with AGILE up to ≈ 3 GeV, including a giant outburst in 2007 prior to the *Fermi* launch (Vercellone et al. 2009, 2010). Based on > 100 MeV data taken during the checkout and early science phase of the mission (2008 July 7– October 6), this source was found to be variable on timescales down to $t_v \sim$

few days (Abdo et al. 2009). A well-sampled data set using the ground-based SMARTS (Small and Moderate Aperture Research Telescope System) in the B, V, R, J, and K bands, and the *Swift* X-ray telescope (XRT) and ultraviolet-optical telescope (UVOT) was collected simultaneously with *Fermi* observations in the period 2008 August through December (Bonning et al. 2009). These multiwavelength observations revealed that the infrared, optical, and γ -rays have similar variability patterns. The γ rays display similar relative flux changes compared to the longer optical wavelengths, but smaller relative flux changes as the short wavelength optical emission, which Bonning et al. (2009) interpreted as being due to an underlying accretion disk. The *Swift* X-ray data did not strongly correlate with the other wavelengths, though Jorstad et al. (2010) and Bonnoli et al. (2010) find a correlation at different epochs.

The *Fermi* observations of 3C 454.3 revealed a broken power-law spectrum, with $\Gamma \cong 2.3 \pm 0.1$ (where the photon flux $\Phi \propto E^{-\Gamma}$) and $\Gamma \cong 3.5 \pm 0.25$, below and above a break energy of 2.4 ± 0.3 GeV, respectively (Abdo et al. 2009). This spectrum is not consistent with Compton scattering of a lower-energy photon source by jet electrons in the fast- or slow-cooling regimes, the standard interpretation for the high energy spectrum in leptonic models of blazars. Abdo et al. (2009) also consider it unlikely that the spectral break is a result of $\gamma\gamma$ absorption with a local radiation field or the extragalactic background light (EBL), the former because this would require a lower jet bulk Lorentz factor than that inferred from superluminal radio observations of 3C 454.3 ($\Gamma_{bulk} \approx 15$; Jorstad et al. 2005), and the latter because the universe is transparent to 40 GeV photons at $z \lesssim 1.0$ for all EBL models (e.g., Finke et al. 2010; Stecker et al. 2006; Gilmore et al. 2009). Abdo et al. (2009) thus consider the most likely explanation to be that the spectral break is caused by an intrinsic break in the electron distribution. However, as explained below, this is unlikely, given the broadband spectral energy distribution of this source.

In this letter, we show that a combination of two Compton scattering components can explain the break in the LAT spectrum of 3C 454.3. In particular, we consider a combination of components from Compton-scattered accretion disk and broad-line region (BLR) radiation, both of which should be strong seed photon sources in FSRQs. The implications of this model for the BLR and for the variability of the emitted radiation are explored. Finally, we conclude with a brief discussion, with implications for breaks in other sources.

We use parameters $H_0 = 71 \text{ km s}^{-1} \text{ Mpc}^{-3}$, $\Omega_m = 0.27$, and $\Omega_\Lambda = 0.73$ so that 3C 454.3, with a redshift of $z = 0.859$, has a luminosity distance of $d_L = 5.5 \text{ Gpc}$.

2. The Spectral Energy Distribution of 3C 454.3

The contemporaneous SED data from 3C 454.3 are given in Abdo et al. (2009) and plotted in Fig. 1. The radio data are likely from a larger region of the jet than the rest of the SED, and can be treated as upper limits for the purposes of model fits. We assume that the electron distribution which produces this radiation has the form of a broken power-law given by $n_e \propto \gamma'^{-p_1}$ for $\gamma'_{min} < \gamma' < \gamma'_{brk}$ and $n_e \propto \gamma'^{-p_2}$ for $\gamma'_{brk} < \gamma' < \gamma'_{max}$. The *Swift* UVOT data give a power-law spectrum with $\Gamma_{opt} \approx 2.9$, presumably from electron synchrotron emission. The X-rays from the *Swift* XRT give $\Gamma_X \approx 1.4$, which should be the index of the synchrotron emission below the break, assuming that the X-rays are from Compton-scattering with the same electrons as are causing the lower-energy synchrotron emission. Thus the *Swift* data imply that, if the electron distribution can indeed be represented by a double power-law, $p_1 \approx 1.8$, and $p_2 \approx 4.8$, since $p = 2\Gamma - 1$. This spectrum indicates a fast cooling regime, where one expects $p_1 \approx 2$ and $p_2 = q + 1$, where q is the injection index.

If the LAT spectrum was the result of Thomson scattering of a single source of photons, whether that source is the disk, BLR, or dust torus, the spectral indices would be about the same as for the synchrotron, namely, $\Gamma \approx 1.4$ and $\Gamma \approx 2.9$ well below and above the break, respectively. Instead, $\Gamma \approx 2.3$ and $\Gamma \approx 3.5$ are observed, respectively, although it is possible that Klein-Nishina (KN) effects could soften the higher energy index. The lower energy LAT index furthermore does not necessarily correspond to the asymptotic value at $E \approx E_{br}$.

Abdo et al. (2009) suggested that the break could be caused by the high energy cutoff in the electron distribution, γ_{max} . However, if this is the case, below the γ -ray break, one would expect the same Γ as in the optical ($\Gamma_{opt} = 2.9$), because of their correlated variability, instead of the $\Gamma = 2.3$ which is observed. The γ -ray spectral index could be softer than Γ_{opt} , due to KN effects, but it is unlikely to be harder.

It is possible that the X-rays through *Fermi* γ -rays are all created by a single component, likely the SSC component, since this is generally broader than external Compton components. In this model, the softer γ -rays are created by the portion of the SSC component at and below the break, as it gradually softens. This SSC-only model gives an adequate fit to the broadband SED, although it gives a poor fit to the LAT data (Fig. 1), and does not produce a sharp break in the LAT γ -ray spectrum, although Abdo et al. (2009) found that the LAT spectrum could just as easily be fit by a smooth transition such as, for example, a power-law with an exponential cutoff. See Table 1 for the spectral parameters for this fit and Finke et al. (2008) for details on this model. The SSC-only model in Fig. 1 does not enter the KN regime until around $\nu \gtrsim 3 \times 10^{26}$ Hz, which is considerably above the *Fermi*-LAT data, and these γ -rays are thus produced entirely in the Thomson regime. However, it is possible that local $\gamma\gamma$ absorption could soften the higher energy portion of the spectrum and

produce a better fit.

But the SSC model has other problems. It ignores the BLR for this source, which must be present due to the strong broad emission lines seen in this object’s optical spectrum; it results in an extremely low magnetic field, B , which is considerably lower than the equipartition value, B_{eq} , and thus the particle jet power, $P_{j,par}$ is much greater than the magnetic field jet power, $P_{j,e}$ and close to the Eddington limit (see Table 1); and it may not be consistent with the variability of this source (see § 5 below). The constraints on the Doppler factor from Jorstad et al. (2005) and the constraints on the emitting region size from the variability timescale imply $B = 0.032 \pm 0.005$ G for the SSC model. We propose that the LAT spectrum of 3C 454.3 is instead the result of a combination of two Compton-scattered components, for example, Compton scattering of the disk and BLR radiation.

3. BLR Radiation Energy Density

Before modeling the SED of 3C 454.3, we derive approximate formulae for the energy density of the BLR at the location of the jet. A regime where the energy densities of the Compton-scattered disk and BLR components are approximately equal can explain the LAT spectrum of 3C 454.3.

We assume that the BLR is spherically symmetric and extends from inner radius R_i to outer radius R_o , and the electron number density of the BLR is a function of distance from the central source, $n_{BLR}(R) = n_0(R/R_i)^\zeta$, so that the Thomson depth of the BLR is given by $\tau_{BLR} = \sigma_T \int_{R_i}^{R_o} dR n_{BLR}(R)$ giving, when $R_i \ll R_o$,

$$\tau_{BLR} \cong \sigma_T n_0 \begin{cases} \frac{R_o}{\zeta+1} \left(\frac{R_o}{R_i}\right)^\zeta, & \zeta > -1 \\ \frac{-R_i}{\zeta+1}, & \zeta < -1 \end{cases}. \quad (1)$$

The BLR Thomson-scatters photons from the accretion disk, assumed to be a point source located at origin with luminosity L_d . If the distance from the black hole to the γ -ray emitting region, $r < R_i$, the energy density from BLR radiation is approximately independent of r , so

$$u_{BLR}(r < R_i) \cong \frac{L_d \sigma_T}{4\pi c} \int_{R_i}^{R_o} \frac{dR}{R^2} n_{BLR}(R) \\ \cong \frac{L_d \tau_{BLR}}{4\pi c} \begin{cases} \frac{1}{R_i^2} \frac{\zeta+1}{\zeta-1}, & \zeta < -1 \\ \frac{1}{R_i R_o} \left(\frac{R_i}{R_o}\right)^\zeta \frac{\zeta+1}{\zeta-1}, & -1 < \zeta < 1 \\ \frac{1}{R_o^2} \frac{\zeta+1}{\zeta-1}, & \zeta > 1 \end{cases}, \quad (2)$$

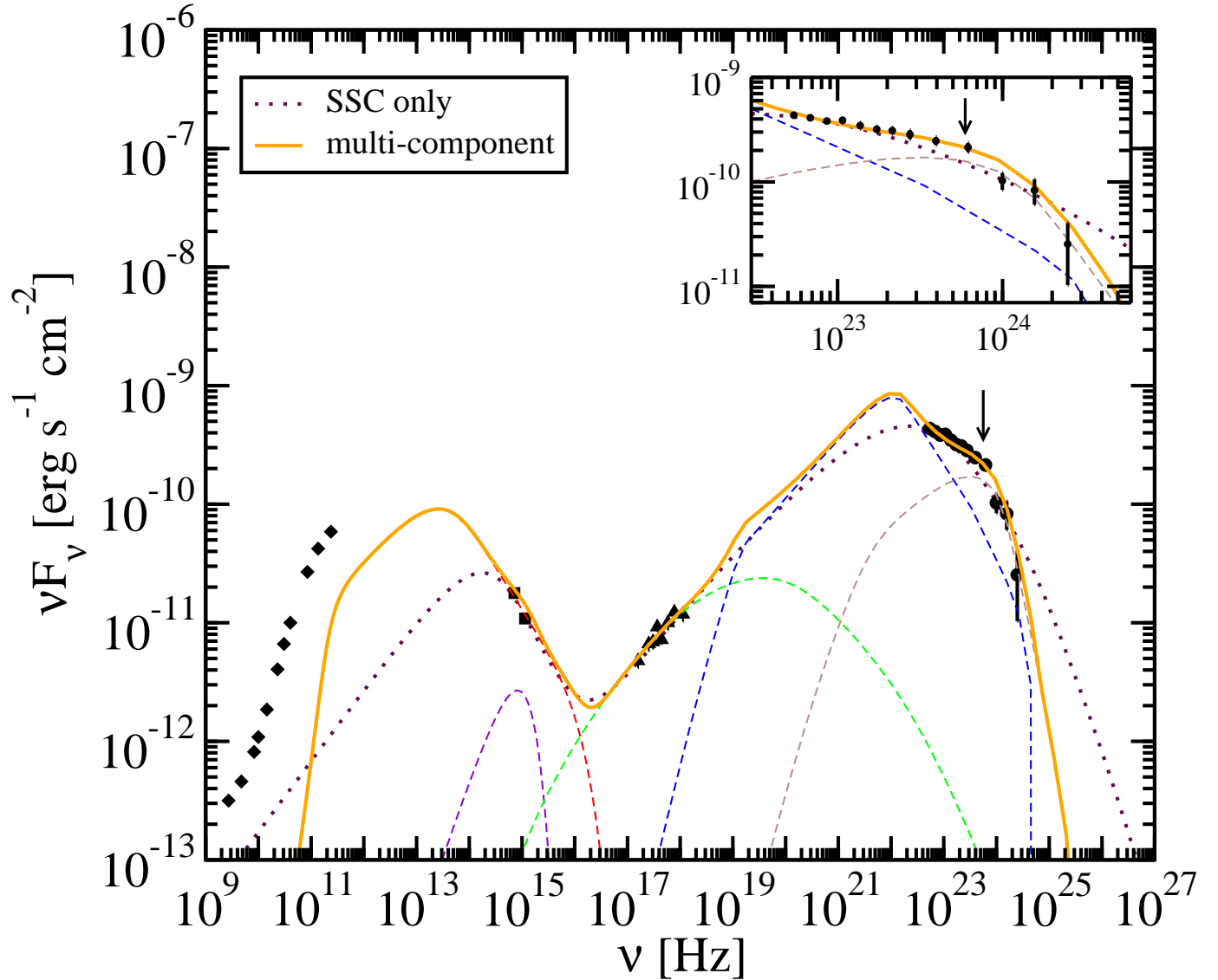


Fig. 1.— The SED of 3C 454.3. The Effelsberg/IRAM radio data are given by the diamonds, the *Swift*-UVOT and XRT data are given by the squares and triangles, respectively, and the *Fermi*-LAT data by the filled circles. The model components for the multi-component model are shown as dashed curves, where the purple dashed curve is the Shakura-Sunyaev disk, the red is the synchrotron, the green is the SSC, the blue is the Compton-scattered disk, and the brown is the Compton-scattered BLR component assuming $\tau_{BLR} = 0.01$. The thick dotted curve gives the SSC fit, and the thick solid curve shows the multi-component model. The inset shows the *Fermi*-LAT spectrum in more detail. The arrows indicate the frequency of the spectral break.

Table 1. Model Parameters¹.

Symbol	Multi-Component model	SSC model
z	0.859	0.859
Γ_{bulk}	15	15
δ_D	30	15
B	0.4 G	0.032 G
t_v	1.7×10^5 s	1.7×10^5 s
p_1	2.0	1.8
p_2	4.4	4.8
γ'_{min}	3×10^1	10
γ'_{max}	2×10^4	2×10^9
γ'_{brk}	1.1×10^3	10^4
M_g	2.0	
l_{Edd}	0.04	
η	1/12	
r	$1.5 \times 10^3 R_g$	
τ_{BLR}	0.01	
R_i	$5.0 \times 10^2 R_g$	
R_o	$5.0 \times 10^5 R_g$	
ζ	-2	
B/B_{eq}	0.6	0.06
$P_{j,B}$	1.8×10^{45} erg s ⁻¹	10^{43} erg s ⁻¹
$P_{j,par}$	2.7×10^{46} erg s ⁻¹	2.3×10^{47} erg s ⁻¹

¹See text and Dermer et al. (2009) for details on parameters and calculations of jet powers.

using eqn. (1). If $R_i < r < R_o$, then, assuming the logarithm term in eqn. (93) of Dermer et al. (2009) is ≈ 1 ,

$$u_{BLR}(r) \cong \frac{L_d \sigma_T}{4\pi c r} \int_{R_i}^{R_o} \frac{dR}{R} n_{BLR}(R)$$

$$\cong \frac{L_d \tau_{BLR}}{4\pi c} \begin{cases} \frac{1}{r R_i} \left(\frac{r}{R_i}\right)^\zeta \frac{\zeta+1}{\zeta}, & \zeta < -1 \\ \frac{1}{r R_o} \left(\frac{r}{R_o}\right)^\zeta \frac{\zeta+1}{\zeta}, & -1 < \zeta < 0 \\ \frac{1}{R_i R_o} \left(\frac{R_i}{R_o}\right)^\zeta \frac{\zeta+1}{\zeta-1}, & 0 < \zeta < 1 \\ \frac{1}{R_o^2} \frac{\zeta+1}{\zeta-1}, & \zeta > 1 \end{cases} . \quad (3)$$

(see also Donea & Protheroe 2003).

4. Compton Scattering Disk and BLR Radiation

The external Compton-scattered BLR νF_ν flux in the Thomson regime can be approximated as

$$f_\epsilon^{ECBLR} = \frac{\delta_D^6}{6\pi d_L^2} c \sigma_T u_{BLR} \tilde{\gamma}'^3 N_e(\tilde{\gamma}') \quad (4)$$

where $\tilde{\gamma}' = \sqrt{\epsilon(1+z)/[\delta_D^2 \epsilon_d(8.4r_g)]}$ (Dermer & Schlickeiser 1994) and ϵ is the observed photon energy. For 3C 454.3, $\Gamma_{bulk} \approx 15$, the Doppler factor $\delta_D \approx 25$ (Jorstad et al. 2005). Gu et al. (2001) found $M_9 = M_{BH}/(10^9 M_\odot) \approx 4.4$ where M_{BH} is the black hole mass. A more recent analysis of the black hole mass gives $M_9 = 1 - 3$ (Bonnoli et al. 2010), and we assume for the remainder of this work that $M_9 = 2$. If the γ -ray emission region is located at $r \ll \Gamma_{bulk}^4 r_g \approx 10^2$ pc, where $r_g = GM_{BH}c^{-2} = 1.5 \times 10^{14} M_9$ cm, then the external Compton-scattered disk emission is in the near field regime. In this case the received νF_ν flux can be approximated by

$$f_\epsilon^{ECD} = \frac{\delta_D^6}{2} \frac{c \sigma_T}{6\pi d_L^2} \left[\frac{L_d r_g}{4\pi r^3 c} \right] \bar{\gamma}'^3 N_e(\bar{\gamma}') , \quad (5)$$

where $\bar{\gamma}' = 2\sqrt{(1+z)\epsilon/[\delta_D^2 \epsilon_d(\sqrt{3}r)]}$ (Dermer & Schlickeiser 2002). Here

$$\epsilon_d(R) = 1.5 \times 10^{-4} \left[\frac{l_{Edd}}{M_9 \eta} \right]^{1/4} \left(\frac{R}{r_g} \right)^{-3/4}$$

is the mean photon energy from a Shakura & Sunyaev (1973) accretion disk at R , $l_{Edd} = L_d/L_{Edd}$, $L_{Edd} = 1.3 \times 10^{47} M_9$, and η is the accretion efficiency.

A solution where the Compton-scattered disk and BLR emission are approximately equal can explain the *Fermi*-LAT emission. Also, a robust solution is obtained by noting that both f_{ϵ}^{ECBLR} and f_{ϵ}^{ECD} are $\propto r^{-3}$ if $\zeta = -2$ and $R_i < r < R_o$. A BLR gradient of $\zeta = -2$ is consistent with a wind model (Murray & Chiang 1995; Chiang & Murray 1996). Setting eqns. (4) and (5) equal to each other, and, ignoring the fact that the electrons generally scatter photons of different energies, one obtains the condition $\tau_{BLR} = (R_i/r_g)^{-1}$ for emission regions formed in the BLR. In order to have comparable flux from the two components, this relation shows that the total Thomson depth through the wind should increase in inverse proportion to the inner radius of the BLR.

An accurate fit to the multiwavelength SED using the multi-component model of Dermer et al. (2009), using model parameters from Table 1 with $\tau_{BLR} = 0.01$, is seen in Fig. 1. In this model, the portion of the *Fermi* spectrum below the break is from Compton scattering of a combination of direct accretion disk and BLR-reprocessed radiation, while above the break it is almost entirely from Compton scattering of BLR-reprocessed disk photons. This model uses the full Compton cross section for all Compton calculations, and the full Shakura-Sunyaev disk spectrum for both direct and BLR-reprocessed Compton-scattered emission. For the Compton-scattered BLR calculation, the Shakura-Sunyaev disk spectrum is assumed to originate from the black hole itself, whereas in the direct disk-scattered calculation, geometric effects are taken into account.

For KN effects to become important in Compton scattering the BLR radiation, $\gamma' \gtrsim (4\Gamma_{bulk}\epsilon_d)^{-1}$ where ϵ_d is the typical dimensionless energy of photons from the disk in the disk's stationary frame. For our model, $\epsilon_d = 2.2 \times 10^{-5}$, and $\Gamma_{bulk} = 15$, so that $\gamma'_{KN} = 760$. Electrons with this energy scatter photons primarily to energies of $\epsilon_{KN} \approx \delta_D^2 \epsilon_d \gamma_{KN}^2 / (1+z) = 6.2 \times 10^3$ which corresponds to frequencies of $\nu = 7.6 \times 10^{23}$ Hz. Thus above the break the Compton scattering of the BLR is almost entirely in the KN regime. Since the KN cross section goes as approximately $\sigma_{KN} \propto \epsilon^{-1}$, f_{ϵ}^{BLR} should go as $\Gamma \approx \Gamma_{opt} + 1 = 3.9$ above the break in the γ -ray spectrum. This is quite close to the $\Gamma = 3.5$ which is observed by *Fermi*. Although the BLR photons are Thomson-scattered disk photons with essentially the same energy as the direct disk photons, geometric effects from Doppler boosting and aberration make Compton-scattered BLR radiation peak at higher photon energies than the disk photons, which tend to come from behind.

The threshold for $\gamma\gamma$ absorption from the BLR-reprocessed disk radiation implies that γ -rays with energies $\epsilon \gtrsim 2[\epsilon_d(8.4r_g)(1+z)]^{-1}$ will be absorbed. For our model this turns out to be $\epsilon \approx 4.9 \times 10^4$ or $\nu \approx 6.0 \times 10^{24}$ Hz, which is above the highest energy photon observed with the *Fermi*-LAT from this source.

The sum of the particle and magnetic-field power $P_{j,par} + P_{j,B}$ is well below $L_{Edd} =$

2.6×10^{47} erg s⁻¹ for $M_9 = 2.0$ (the photon power is $\approx 8 \times 10^{46}$ erg s⁻¹). The model is close to equipartition between the total particle and magnetic-field energy densities, assuming a factor $10\times$ more energy in total nonthermal particles than electrons, i.e., $P_{j,par} = 10P_{j,e}$. Our multi-component fit has lower jet power than the fit to the same SED by Ghisellini et al. (2009), due primarily to their assumption of a larger proton power, with $P_{j,par} > 200 \times P_{j,e}$.

5. Variability

The γ -ray spectral break observed with *Fermi* was constant over several month timescales (Abdo et al. 2009). As the γ -ray-emitting region moves outward, the spectral break should remain at approximately the same energy, since for $\zeta = -2$, the BLR- and disk-scattered flux should remain approximately equal. The overall γ -ray flux will, of course, change over time, but as long as $R_i < r \ll \Gamma^4 r_g$, and R_i or τ_{BLR} does not change significantly, the γ -ray spectral break should be present.

In Bonning et al. (2009), optical observations are seen to vary with changes on the same magnitude as the γ -rays. If the γ -rays were produced by SSC emission, “quadratic variability”, i.e., $f_\epsilon^{SSC} \propto (f_\epsilon^{syn})^2$, might be expected. The absence of such variability is in accord with our spectral fitting results means that this model for 3C 454.3 is disfavored.

The X-ray light curve of 3C 454.3 shows little variability during this time, and is not correlated with the IR, optical, UV, or γ -rays (Bonning et al. 2009). This can be explained by the longer cooling timescale (see Fig. 2). These timescale calculations use monochromatic approximations for the Compton-scattered disk and BLR components, but the full Compton cross section for all components. The electrons which make the X-rays by SSC have lower energies than those that make the optical and γ -rays, and thus cool more slowly than the observed variability timescale.

The lack of correlated variability between X-rays and optical and γ -rays might indicate that the X-rays originate from another part of the jet than the LAT γ -rays. However, in this case, the emission would still likely be in the fast cooling regime, since the γ -ray flux is significantly greater than the optical and radio fluxes, and as long as one is in the fast cooling regime, Compton scattering of a single component cannot explain the LAT spectrum. Furthermore, during the 2007 November flares of 3C 454.3, detected by *Swift* UVOT, XRT and BAT, *INTEGRAL*, and *AGILE*, the X-rays were weakly variable, compared with other wavebands, but did seem to show correlated variability (Vercellone et al. 2009), which indicates they originate from the same emission region. One final possibility is that a hadronic model may be possible to explain the LAT γ -ray spectrum (e.g., Mücke & Protheroe

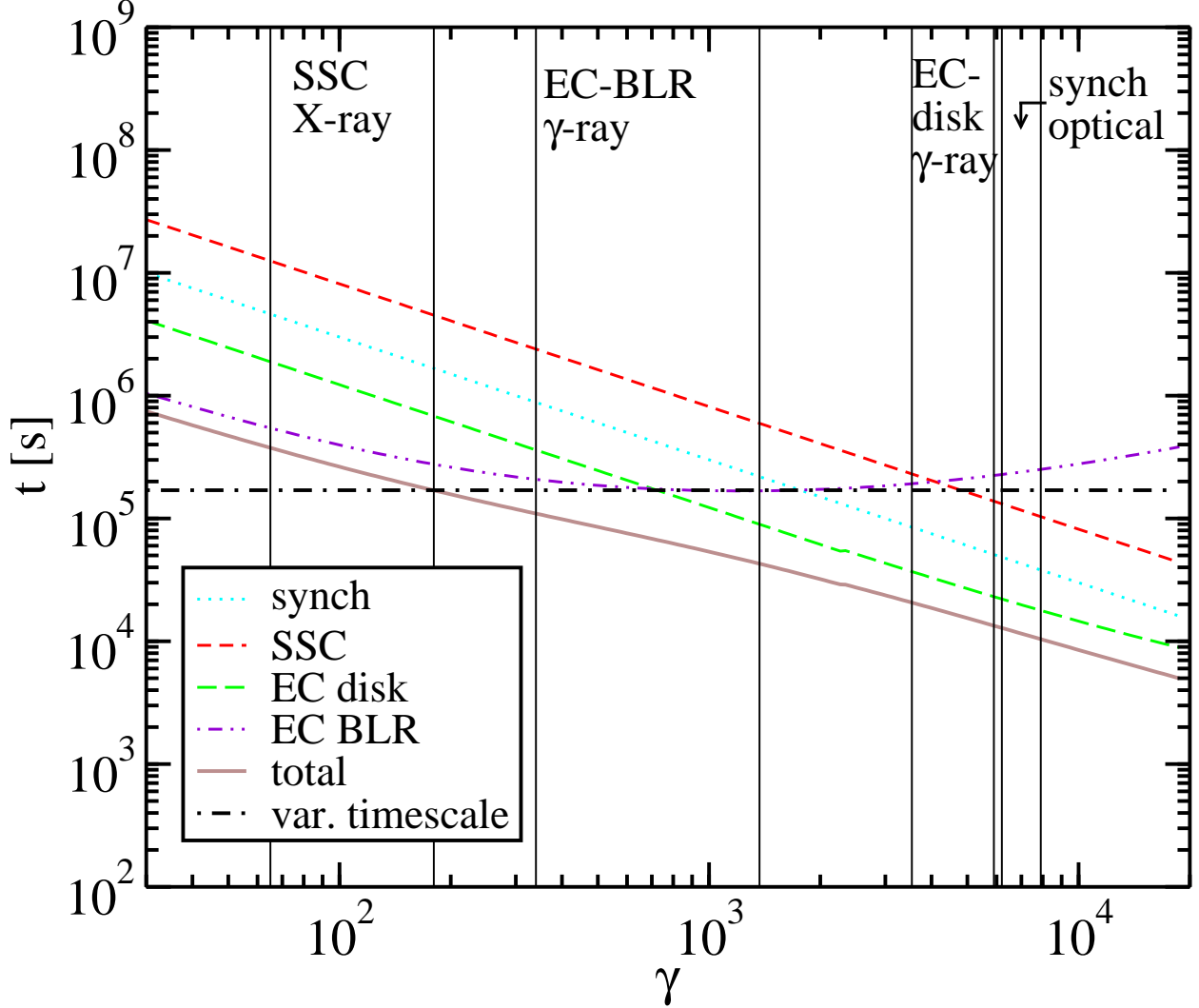


Fig. 2.— Cooling timescales in the observer’s frame. The electrons with γ which produce the majority of the radiation in certain wavebands are marked. The electrons which produce X-rays from SSC emission have total cooling timescales longer than the variability timescale, explaining the lack of X-ray variability. The optical synchrotron radiation is made by electrons with $\gamma \approx 6\text{--}8 \times 10^3$, which would therefore correlate with the γ rays formed by Compton-scattered disk radiation.

2001), however, such models may have difficulties in explaining the correlated variability seen in this source, since protons would evolve on longer timescales than electrons.

6. Discussion

Assuming the dual-component Compton-scattering scenario presented in this paper is correct, what can it tell us about the location of the γ -ray emission region? It implies that this region is $R_i < r \ll \Gamma^4 r_g$, so that, using the parameters from the modeling of 3C 454.3, the location of the jet falls over a large range from $0.1 \text{ pc} < r \ll 100 \text{ pc}$. However, the external energy density from disk and BLR radiations is $\propto r^{-3}$, a steep decline, so that the blob must be within $\approx 0.1 \text{ pc}$ for a significant scattering component. Recent modeling of 3C 454.3 (Bonnoli et al. 2010) also finds that the γ -ray emitting region is within the BLR. By contrast, Sikora et al. (2008) suggested that the γ -rays observed by EGRET and AGILE were caused by Compton-scattering of radiation from hot dust by a blob located $\sim 10 \text{ pc}$ from the central black hole, though detailed modeling is still needed to determine if this model can explain the sharp spectral break in the *Fermi* observations. The blazar 3C 279 also shows a similar spectral break during the onset of an extended episode of optical polarization, while the jet emission region could still be within the BLR region (Abdo et al. 2010a).

Whether this model can predict similar spectral breaks in other FSRQs and low-synchrotron-peaked blazars, such as AO 0235+164 or PKS 1502+106 (Abdo et al. 2010b), depends mainly on the properties of the BLR in these sources, in particular, whether $\tau_{BLR} \approx r_g/R_i$. In specific blazars, especially at higher z , $\gamma\gamma$ -absorption by scattered disk radiation (Reimer 2007) could still be effective. Detailed modeling of simultaneous SED data will test these scenarios, as it does for the case of 3C 454.3. If our model is correct, it provides evidence for a wind model of the BLR (Murray & Chiang 1995; Chiang & Murray 1996; Elvis 2000).

We are grateful to the anonymous referee for helpful comments. J.D.F. was supported by NASA Swift Guest Investigator Grant DPR-NNG05ED411 and NASA GLAST Science Investigation DPR-S-1563-Y. C.D.D. was supported by the Office of Naval Research.

REFERENCES

- Abdo, A. A. et al. 2009, ApJ, 699, 817
 —. 2010a, Nature, 463, 919

- . 2010b, *ApJ*, 710, 1271
- Bonning, E. W., Baily, C., Urry, C. M., Buxton, M., Fossati, G., Maraschi, L., Coppi, P., Scalzo, R., Isler, J., & Kaptur, A. 2009, *ApJ*, 697, L81
- Bonnoli, G., Ghisellini, G., Foschini, L., Tavecchio, F., & Ghirlanda, G. 2010, *MNRAS*, submitted, arXiv:1003.3476
- Chiang, J. & Murray, N. 1996, *ApJ*, 466, 704
- Dermer, C. D., Finke, J. D., Krug, H., & Böttcher, M. 2009, *ApJ*, 692, 32
- Dermer, C. D. & Schlickeiser, R. 1994, *ApJS*, 90, 945
- . 2002, *ApJ*, 575, 667
- Donea, A. & Protheroe, R. J. 2003, *Astroparticle Physics*, 18, 377
- Elvis, M. 2000, *ApJ*, 545, 63
- Escande, L. & Tanaka, Y. T. 2009, *The Astronomer’s Telegram*, 2328, 1
- Finke, J. D., Dermer, C. D., & Böttcher, M. 2008, *ApJ*, 686, 181
- Finke, J. D., Razzaque, S., & Dermer, C. D. 2010, *ApJ*, 712, 238
- Ghisellini, G., Tavecchio, F., & Ghirlanda, G. 2009, *MNRAS*, 399, 2041
- Gilmore, R. C., Madau, P., Primack, J. R., Somerville, R. S., & Haardt, F. 2009, *MNRAS*, 399, 1694
- Gu, M., Cao, X., & Jiang, D. R. 2001, *MNRAS*, 327, 1111
- Jorstad, S. G. et al. 2005, *AJ*, 130, 1418
- . 2010, *ApJ*, submitted, arXiv:1003.4293
- Mücke, A. & Protheroe, R. J. 2001, *Astroparticle Physics*, 15, 121
- Murray, N. & Chiang, J. 1995, *ApJ*, 454, L105+
- Reimer, A. 2007, *ApJ*, 665, 1023
- Shakura, N. I. & Sunyaev, R. A. 1973, *A&A*, 24, 337
- Sikora, M., Moderski, R., & Madejski, G. M. 2008, *ApJ*, 675, 71

Stecker, F. W., Malkan, M. A., & Scully, S. T. 2006, ApJ, 648, 774

Tosti, G., Chiang, J., Lott, B., Do Couto E Silva, E., Grove, J. E., & Thayer, J. G. 2008,
The Astronomer's Telegram, 1628, 1

Vercellone, S. et al. 2009, ApJ, 690, 1018

—. 2010, ApJ, 712, 405